PHYSICAL REVIEW B **70**, 115111 (2004)

Electric field gradient calculations for Li_xTiS_2 and comparison with ^{7}Li NMR results

Thomas Bredow,[1] Paul Heitjans,[2] and Martin Wilkening[2]
[1]*Theoretische Chemie, Universität Hannover, Am Kleinen Felde 30, 30167 Hannover, Germany*
[2]*Institut für Physikalische Chemie und Elektrochemie, Universität Hannover, Callinstr. 3-3A, 30167 Hannover, Germany*
(Received 17 February 2004; revised manuscript received 2 June 2004; published 27 September 2004)

The elements of the electric field gradient tensor at Li position in the intercalation compound Li_xTiS_2 (with $x=0.25$, 0.33, 0.67, and 1.0) were calculated with first-principles methods and periodic supercell models. The theoretical results obtained with density functional and Hartree-Fock hybrid methods were compared with experimental field gradients extracted from ^{7}Li NMR spectra from the literature and from our measurements presented here. The dependence of calculated field gradients on the basis set and the explicit form of the exchange-correlation density functional was investigated. In agreement with earlier studies a pronounced effect of polarization functions at the Li site was observed. After optimization of internal degrees of freedom in $LiTiS_2$ all methods under consideration give quadrupole coupling constants in close agreement with experiment. For $x<1$ the calculated quadrupole coupling constants were found to depend more sensitively on the method which was attributed to differences in the description of spin localization. The calculations allow one to distinguish between Li atoms placed at octahedral and tetrahedral interstitial sites of the host lattice TiS_2.

DOI: 10.1103/PhysRevB.70.115111 PACS number(s): 71.15.Ap, 71.15.Mb, 71.20.Tx, 82.56.−b

I. INTRODUCTION

The hexagonal modification of the dichalcogenide TiS_2 is one of the best known materials which is suitable for intercalation with guest species. Between the TiS_2 layers empty octahedral and tetrahedral sites can be occupied by guest atoms or molecules. The hexagonal Li intercalation compound h-Li_xTiS_2 (space group $P\bar{3}m1$), where the Li ions are reported to preferentially occupy octahedral sites, has been studied as a promising material for high-energy density batteries.[1–3] It is stable in the entire intercalation range $0<x\leqslant 1$. h-Li_xTiS_2 is a fast two-dimensional lithium ion conductor[2,4] and shows semimetallic properties.[5–7] Recently, also the lithium intercalation in open-ended TiS_2 nanotubes[8] and the Li dynamics in nanocrystalline h-Li_xTiS_2 has been studied.[9–11]

The Li/TiS_2 system has attracted considerable attention from theorists. The structural, elastic, and electronic effects of lithium intercalation in h-TiS_2 were studied with periodic Hartree-Fock (HF) calculations.[12] The electronic structure of lithium-intercalated TiS_2 was analyzed with finite-size cluster models at semi-empirical level and with first-principles methods.[13,14] Ionic relaxation and its effect on the electronic structure of Li intercalated metal dichalcogenides were studied with the *ab initio* pseudopotential method.[15] Order-disorder transitions in Li_xTiS_2 were investigated with a mean-field approach using a triangular lattice gas model.[16] Furthermore, the cubic spinel structures of TiS_2 and $Li_{0.5}TiS_2$ were studied theoretically with first-principles methods based on density-functional theory (DFT).[17]

The elements of the electric field gradient (EFG) tensor, **V**, are a sensitive measure of the local electronic structure in solids and molecular systems. Experimentally, the coupling of the electric field gradient and the quadrupole moment tensor, **Q**, of nuclei with spin quantum number $I\geqslant 1$ is accessible by nuclear magnetic resonance (NMR) techniques.[18–20] First-principles quantum-chemical investigations of quadrupolar interactions in solid systems are based on two kinds of models, the embedded cluster model[21–23] and the periodic supercell model, either based on plane-waves[24–27] or on atom-centered basis functions.[28–30] While periodic models take into account long-range electrostatic interactions in crystalline systems, the results obtained with model clusters strongly depend on their size and shape.[28]

The accuracy of calculated EFG obtained with different quantum-chemical methods were compared by Schwerdtfeger *et al.*[31,32] The HF method, post-HF methods like perturbation theory and coupled-cluster configuration interaction, various DFT methods with and without gradient corrections in the exchange-correlation functional, and hybrids between HF and DFT were compared. The EFG was found to be sensitive to the specific form of density functional used. Field gradients obtained with pure DFT methods both with and without gradient corrections were found to deviate from the other methods. It was concluded that current DFT approximations are less accurate than HF-based methods. This agrees with a part of the literature,[33] but other studies come to the opposite conclusion, in particular for main-group elements.[34,35]

The aim of the present study is to investigate the reliability of DFT and HF-DFT hybrid approaches for the prediction of EFG at the Li site in Li_xTiS_2 using periodic supercell models. Here we have focused on the hexagonal modification. Lithium is placed both at octahedral and tetrahedral sites of the layered h-TiS_2 lattice with various mole fractions x, ranging from 0.25 to 1.0. The theoretical results are compared to experimental data from the literature and from our NMR measurements. Whereas a number of NMR studies focus on the Li dynamics in h-Li_xTiS_2,[4,9–11,36–39] there are only few experimental NMR investigations available studying static properties.[36,39–41] Since there exist discrepancies for experimental data of the quadrupole coupling constant, in particular for $x<1$, between earlier measurements[36,39] and more recent investigations,[41] we have performed comple-

mentary NMR measurements for h-Li_xTiS_2 with various Li contents x. For instance, the values for the quadrupole coupling constant which can be found in the literature for h-$Li_{0.7}TiS_2$ differ by about 50%. Furthermore, in Ref. [41] the EFG tensor is reported to be not axial symmetric for h-$Li_{0.7}TiS_2$ and h-$Li_{1.0}TiS_2$, whereas earlier investigations with continuous wave NMR (Ref. 39) indicate an axial symmetric EFG tensor.

The paper is organized as follows: In Sec. II experimental details are briefly described and our NMR results complementary to those reported in the literature are presented. In Sec. III we describe the computational methods used for our calculations, in Sec. IV we discuss the calculated results in comparison with experimental values.

II. EXPERIMENTAL DETAILS AND NMR RESULTS

A. Experiment

The lithium intercalated hexagonal TiS_2 samples used here for supplementary measurements of ^{7}Li NMR spectra are identical to those used for frequency dependent ^{7}Li NMR relaxation studies[4] by our group before. The intercalation was done chemically with n-butyl lithium in hexane. Details of sample preparation which had been performed by Payer and Schöllhorn are given in Ref. 42.

^{7}Li ($I=3/2$) NMR spectra of hexagonal Li_xTiS_2 ($x=0.3$, 0.7, 1.0) were recorded with a modified Bruker MSL 100 spectrometer connected to a tunable Oxford cryomagnet (0–8 T). The spectra were acquired at resonance frequencies of 32 MHz and 78 MHz, respectively. The $\pi/2$ pulse lengths ranged from 3.5 to 5.5 μs ensuring that both the central ($|1/2\rangle \leftrightarrow |-1/2\rangle$) and the satellite transitions ($|3/2\rangle \leftrightarrow |1/2\rangle, |-1/2\rangle \leftrightarrow |-3/2\rangle$) were excited nonselectively. Recycle delay times were about five times the spin-lattice relaxation time T_1, which is about 11 s at 143 K (rigid lattice regime) and about 3 s at 373 K (regime of extreme narrowing) almost independent of the resonance frequency. T_1 depends only slightly on the Li content.[4]

B. NMR results

1. $Li_{1.0}TiS_2$

Experimental ^{7}Li NMR powder spectra of $Li_{1.0}TiS_2$ in the rigid lattice regime at 158 K and intentionally at 373 K, where motional narrowing is almost completed, are shown in Fig. 1 on the left-hand side. The full spectrum at 373 K is composed of a central transition and two clearly visible inner satellite transitions with their corresponding wings being slightly visible only. The spectra are affected by quadrupole, chemical shift and dipole-dipole interactions. The latter, in particular, are temperature dependent and are averaged at elevated temperatures when jump rates reach the order of the inverse line width (motional narrowing). The spectra can be described by first order perturbation theory. Assuming the same principle axis frame for the quadrupole (q) and chemical shift (cs) interactions, the NMR spectra were calculated (right-hand side of Fig. 1) from the sum of the two relevant

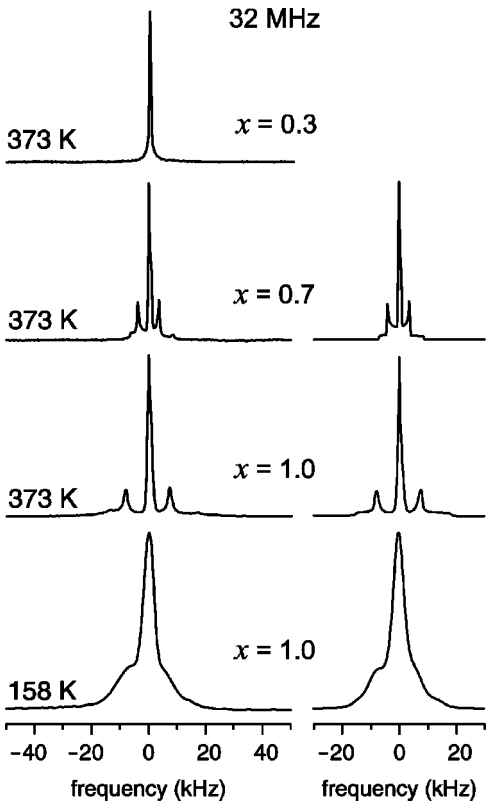

FIG. 1. Experimental ^{7}Li NMR spectra (left-hand side) of h-$Li_{1.0}TiS_2$ at 32 MHz for two different temperatures, i.e., at 158 K (rigid-lattice spectrum) and at 373 K, where the spectrum is substantially narrowed, indicating fast motion of the lithium cations (motional narrowing regime). For comparison spectra with $x=0.7$ and 0.3 at 373 K are displayed, too. The corresponding simulations ($\eta_{cs}=\eta_q=0$; identical axis system) for $x=1.0$ and $x=0.7$ are given on the right-hand side. For h-$Li_{1.0}TiS_2$ a chemical shift anisotropy $|\Delta\sigma|$ of about 50(5) ppm and a quadrupole coupling constant C_q of about 31(2) kHz is obtained from the simulation at 158 K. For h-$Li_{0.3}TiS_2$ C_q is estimated to be less than 5 kHz at 373 K. See text for further details.

interaction Hamiltonians $\hat{H}_q$ and $\hat{H}_{cs}$ (Refs. 19, 20, and 43–45) similar to the simulations in Ref. 41:

$$\hat{H}_q = \frac{1}{4}\frac{e^2qQ}{2I(2I-1)}(3\hat{I}_z - \hat{I}^2)(3\cos^2\theta - 1 - \eta_q \sin^2\theta\cos 2\phi) \tag{1}$$

and

$$\hat{H}_{cs} = -\gamma\hbar B_0 \hat{I}_z \sigma_{iso} + \tfrac{1}{3}B_0\hat{I}_z\Delta\sigma(3\cos^2\theta - 1 - \eta_{cs}\sin^2\theta\cos 2\phi). \tag{2}$$

Here e is the proton charge, eq is the principal component of the field gradient, and $Q=-4.01\times10^{-30}$ m^2 (Ref. 46) is the electric quadrupole moment of ^{7}Li. The angles θ and ϕ describe the orientation dependence in the principle axis frame, furthermore, $\hat{I}$ and $\hat{I}_z$ are the nuclear spin operators. γ is the gyromagnetic ratio of the nucleus, B_0 denotes the external magnetic field, σ_{iso} and $\Delta\sigma=\sigma_{zz}-(\sigma_{yy}+\sigma_{xx})/2$ are the

isotropic chemical shift and the chemical shift anisotropy, respectively. $\eta_q=(V_{xx}-V_{yy})/V_{zz}$ and $\eta_{cs}=(\sigma_{xx}-\sigma_{yy})/\delta_{cs}$ are the asymmetry parameters of the quadrupole interaction and the chemical shift, respectively. V_{xx}, V_{yy}, and V_{zz} are elements of the traceless electric field gradient tensor $\mathbf{V}$. $V_{zz}=eq$ is the principal component. $\delta_{cs}=\sigma_{zz}-\sigma_{iso}$ denotes the reduced chemical shift anisotropy. The quadrupole coupling constant is given by

$$C_q = eQ/h \cdot V_{zz}, \tag{3}$$

where h is Planck's constant. The broadening of the NMR spectra at lower temperatures by dipole-dipole interactions was taken into account by folding the spectra with a suitable choice of weighted Gaussian and Lorentzian functions. From the convolution parameters a rigid lattice linewidth [FWHM (full width at half maximum)] of about 4 kHz is deduced. Simulated spectra obtained with the program WSOLIDS1 (Ref. 47) are shown on the right-hand side of Fig. 1. The best simulation for $Li_{1.0}TiS_2$ at 373 K is clearly obtained with axially symmetric electric field gradient and chemical shift tensors, i.e., $\eta_q=0$ and $\eta_{cs}=0$. The isotropic chemical shift σ_{iso} has not been measured here. σ_{iso} is reported to be −1 ppm for $Li_{1.0}TiS_2$.[41] The simulation for $Li_{1.0}TiS_2$ at 373 K indicates a chemical shift anisotropy $|\Delta\sigma|$ of 45(5) ppm. For the quadrupole coupling constant C_q, defined by Eq. (3), a value of 29.5(5) kHz at 373 K is obtained. In excellent agreement with the result presented in Ref. 41 a value of 29 kHz for C_q at 293 K is found. The same results for C_q can be gathered from the difference $\Delta\nu_q=3C_q/2I(2I-1)$ (valid for $\eta_q=0$) between the satellite peaks or from the separation of the outer wings. In addition, we recorded high-temperature ^{7}Li NMR spectra up to 723 K. For instance, C_q is 32.4(2) kHz at 673 K and thus shows a small increase between 293 K and 673 K.

The parameters used for the simulation of the rigid lattice NMR spectrum of $Li_{1.0}TiS_2$ at 158 K (Fig. 1), which is broadened by dipole-dipole interactions, are $|\Delta\sigma|=50(5)$ ppm ($\eta_{cs}=0$) and $C_q=31(2)$ kHz ($\eta_q=0$). NMR spectra between 143 K and 373 K (at 32 and 78 MHz, cf. partly Fig. 2) can be simulated with the same set of parameters indicating that C_q is nearly temperature independent as shown in Ref. 41 for the temperature range 100–298 K. In general the temperature dependence of the coupling constant has to be taken into account when comparing experimental values with computational results calculated for low temperatures. Since it seems probable that the coupling constant remains essentially temperature independent also below 100 K, a straightforward comparison with theoretical values can be made.

Acceptable simulations of the spectra at very low temperatures could also be obtained using values of $\eta_q \leqslant 0.3$. An η_q between 0 and 0.3 has only small effects on the simulations for low temperatures due to dominating dipole-dipole broadening. Our simulations of the rigid lattice NMR spectra show that C_q varies only little with $\eta_q \leqslant 0.3$. These variations of C_q are already covered by the given error range of ±2 kHz, see above. At higher temperatures no evidence was found that the electric field gradient tensor is not axially symmetric as one can clearly see regarding, e.g., the experimental spectrum at 373 K (Fig. 1). A detailed interpretation of a possible temperature dependence of η_q below room temperature is beyond the scope of the present study.

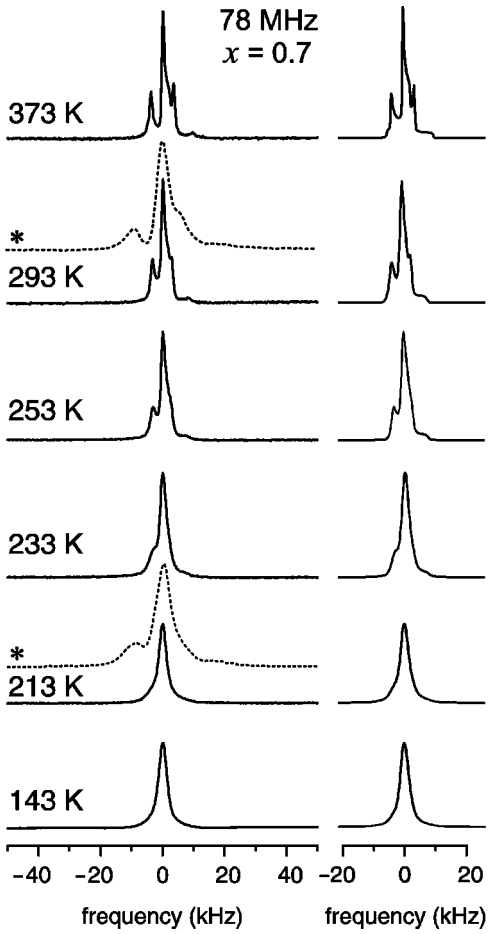

FIG. 2. Experimental ^{7}Li NMR spectra of h-$Li_{0.7}TiS_2$ at 78 MHz for various temperatures (143 K–373 K) on the left-hand side with their corresponding simulations ($\eta_{cs}=\eta_q=0$; identical axis system) on the right-hand side. The quadrupole coupling constant C_q is reduced from 14.8(5) kHz at 373 K to about 12(1) kHz at 213 K. The spectra exhibit a chemical shift anisotropy $|\Delta\sigma|$ of about 24(3) ppm. For comparison spectra of h-$Li_{1.0}TiS_2$ (dotted lines, marked each with an asterisk) at 213 and 293 K are shown, too. See text for further details.

2. $Li_{0.7}TiS_2$

The NMR spectrum of $Li_{0.7}TiS_2$ at 373 K is shown in Fig. 1 for comparison with the spectrum of $Li_{1.0}TiS_2$ at the same temperature. The corresponding simulation with $\eta_{cs}=0$ and $\eta_q=0$ is displayed on the right-hand side of Fig. 1. In comparison to the results of $Li_{1.0}TiS_2$, for $Li_{0.7}TiS_2$ the chemical shift anisotropy $|\Delta\sigma|$ and the quadrupole coupling constant C_q were found to be reduced to 24(3) ppm (in good agreement with Ref. 41) and to 14.8(5) kHz, respectively. Again, the same value of C_q can be obtained from the separation of the two sharp satellite lines.

The NMR parameters of the different interactions at low temperatures are more difficult to extract from experimental

NMR spectra due to dipolar line broadening and, as a consequence thereof, a decrease of the satellite peak intensities. On the left-hand side of Fig. 2 experimental spectra of $Li_{0.7}TiS_2$ at various temperatures are shown with their corresponding simulations ($\eta_q=0$ and $\eta_{cs}=0$) on the right-hand side. Whereas the spectrum at 213 K is still somewhat structured, between 213 K and 143 K additional broadening and decrease of the satellite intensities shows up which leads to unstructured NMR spectra. In agreement with Ref. 41 the rigid lattice line width at 143 K is about 2 kHz. Whereas no clear temperature dependence between 143 K and 373 K is observed for the chemical shift anisotropy, the quadrupole coupling constant slightly decreases with decreasing temperature. C_q is reduced from 14.8(2) at 373 K to 12.6(2) kHz at 293 K (in agreement with Ref. 41) and to about 12(1) kHz at 213 K. C_q is estimated to be about 11(2) kHz at 143 K.

As obvious from the line shapes between 293 K and 373 K, the electric field gradient tensor is clearly axially symmetric. For low temperatures a value of $\eta_q \leqslant 0.2$ can be considered, but with minor effect on the coupling constant. NMR spectra of $Li_{1.0}TiS_2$ at 78 MHz are shown in Fig. 2 (dotted lines), too, in order to emphasize the significant difference in C_q (and $|\Delta\sigma|$) for $x=0.7$ and $x=1.0$.

3. $Li_{0.3}TiS_2$

For $Li_{0.3}TiS_2$ the satellite transitions are not clearly separated from the central transition even in the range of extreme narrowing (cf. Fig. 1). At the bottom of the spectrum at 32 MHz a small additional broadening is observed. The full spectrum can be fitted with a sum of two Lorentzian functions with linewidths (FWHM) of 0.52(2) kHz and 5.7(8) kHz, respectively. The quadrupole coupling constant is estimated to be less than 5 kHz.

III. COMPUTATIONAL METHODS

The tensor components of the electric field gradient **V** were calculated with first-principles methods and periodic supercell models using the crystalline orbital program CRYSTAL03.[48] Here the crystalline orbitals are linear combinations of Bloch functions which are based on atom centered Gaussian-type orbitals. In earlier studies a pronounced basis set dependence of calculated Na EFG for bulk $NaNO_2$ had been found.[28] Therefore we performed a basis set optimization for $LiTiS_2$. The following basis sets (in the Pople notation[49]) served as starting points for our investigation: 8-6411G31*d* for Ti,[50] and 8-6311G* for S.[51,52] Three basis sets from the literature were considered for Li, 6-11G,[12,53] 7-11G,[54] and a fully uncontracted basis.[55]

Three quantum-chemical methods were compared; (a) the Perdew-Wang Generalized Gradient Approximation (PWGGA) of DFT;[56] (b) a HF-DFT hybrid approach (HFPW), where the electron exchange term is a linear combination of the Perdew-Wang functional (0.8) and the exact HF term (0.2) and electron correlation is treated with the Perdew-Wang functional; and (c) the HF method, combined with the Perdew-Wang correlation functional (HF+PW). In an earlier study it was shown that the HFPW hybrid approach reproduces well experimental data on energetic, structural and electronic properties of various metal oxides.[57]

Strict values for the thresholds were used in the calculation of overlap, Coulomb and exchange integrals, 10^{-9}, 10^{-9}, 10^{-9}, 10^{-9}, and 10^{-18}.[48] For the wave function calculations, a self-consistent field (SCF) energy convergence criterion of 10^{-7} a.u. was used. In the numerical integration in reciprocal space the shrinking factors 12 and 24 were used for the Monkhorst and Gilat nets, respectively.[48]

The theoretical quadrupole coupling constant C_q is obtained from the calculated principal EFG tensor component V_{zz} using Eq. (3). The calculated EFG is converted from a.u. to SI units by the factor 9.717×10^{21} V/m^2. This gives an overall factor of 9.634×10^3 for the conversion from V_{zz}(a.u.) to C_q(kHz) in the case of Li. No correction by, e.g., a Sternheimer factor γ_∞, as necessary for point charge models,[58] is applied. In the present quantum-chemical calculations the polarization of the considered ion (Li^+) in the electric field of the surrounding charges and the overlap of the valence shells of the ion with the charge distributions of the neighboring ions are fully taken into account.

IV. RESULTS AND DISCUSSION

A. Basis set convergence

In a previous *ab initio* HF and DFT study of crystalline $NaNO_2$ (Ref. 28) a pronounced basis set dependence of the calculated EFG at sodium position from the atomic basis sets was found. For this reason we tested several basis sets for sulfur and lithium for the calculation of field gradients for $LiTiS_2$ in this study. In the test calculations Li was placed at the octahedral interstitial sites [Fig. 3(a)] and the experimental lattice parameters[59] were taken.

In Table I only the principal EFG component along the *c* axis $V_{cc}=V_{zz}$ is presented. At the high-symmetry Li position for $x=1$, the other diagonal elements of the traceless tensor **V**, V_{aa} and V_{bb}, are equal to $-V_{cc}/2$.

A 8-6411G31*d* basis set[50] was used throughout for Ti. It was assumed that the Ti basis has little effect on the electric field gradient at Li position since the Ti-Li distances (>3 Å) are relatively large. Due to the anionic character of sulfur in $LiTiS_2$, its atomic basis set must be flexible enough to describe the extra electrons. Therefore the 8-6311G* basis set (A) from the literature[52] was augmented by *sp* and *d* shells leading to 8-63111G* and 8-63111G(2*d*) basis sets (B and C in Table I). The inner 1*s*, 2*sp*, and 3*sp* shells remained unchanged while the orbital exponents of the diffuse shells were optimized at UPWGGA level (Table II). Since the EFG was calculated at the Li position, particular care was taken for the choice of the lithium basis set. Three different basis sets from the literature were used as starting points for the convergence study. The 6-11G basis was optimized for Li+ in LiO(OH).[53] A larger contraction for the inner 1*s* shell was used in the DZVP2 or 7-11G basis (D) of Godbout *et al.*[54] A fully uncontracted basis consisting of 18*s* shells[55] was modified by removing the two outermost shells and augmenting the remaining three most diffuse *s* shells with *p* shells (E).

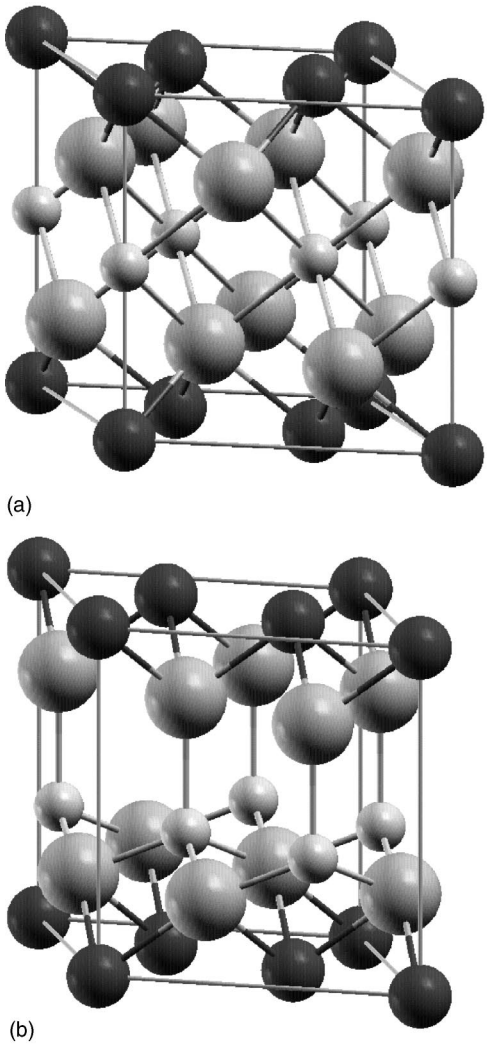

FIG. 3. Primitive unit cell of $LiTiS_2$ with Li intercalated at octahedral (a) and tetrahedral (b) position; medium-size dark circles: Ti, large gray circles: S, small gray circles: Li.

The removal of the diffuse functions was necessary to overcome SCF convergence problems with CRYSTAL03. The *p* functions were added to make this basis more comparable to the 7-11G basis. Finally, basis set (D) was augmented by a *d* shell leading to basis set (F) in order to investigate the effect of polarization functions.

The total energy per unit cell of *h*-$LiTiS_2$ with experimental structure [$a=3.4590$ Å, $c=6.1879$ Å, $z_S=0.238$ (Ref. 59)] at U-PWGGA level was used as convergence criterion. Here U denotes that the unrestricted Kohn-Sham method was used.

The lattice energy was calculated with respect to the free atoms in their corresponding ground states. Convergence of the atomic energies was achieved by adding diffuse *sp* and *d* shells to the above mentioned basis sets. This procedure lead to 6-11111G(2*d*), 7-11111G(2*d*), and 13-11111G* basis sets for the Li atom, to a 8-6311111G(3*d*) basis for S and to a 8-6411111G3111d basis for Ti.

An extension of the S basis set (A) has a considerable effect on the *h*-$LiTiS_2$ lattice energy (Table I). E_L is increased by 14 kJ/mol due to the addition of an *sp* shell with basis (B), and by another 12 kJ/mol after addition of a *d* shell, basis (C). At the same time the field gradient V_{zz} is only changed by 2×10^{-4} a.u. (Table I). The Li basis set has a smaller effect on the energy with changes of E_L ranging from 3 to 6 kJ/mol, basis sets (C)–(F), but has a pronounced effect on the calculated EFG. When the description of the inner 1*s* function is improved by increasing the contraction from 6 to 7 (D), the absolute value of V_{zz} is increased by 29%. A further improved description of the 1*s* orbital by basis (E), however, does not lead to significant changes in the calculated EFG. Since this basis set considerably increases the computational cost, the effect of an additional *d* function was tested with the smaller basis (D). When the 7-11G Li basis is augmented with a *d* shell (F), the calculated field gradient is increased by 55%. The quadrupole coupling constant obtained from V_{zz} using Eq. (3) increases from 21 to 33 kHz which considerably improves the agreement with the measured values ranging from 29 (Ref. 41) to

TABLE I. Basis set dependence of the lattice energy E_L (kJ/mol), the electric field gradient V_{zz} at Li_{oct} position (a.u.$\times10^3$), and quadrupole coupling constant C_q (kHz) of *h*-$LiTiS_2$ with experimental lattice parameters at the PWGGA level.

Basis set	Ti[a]	S[b]	Li	E_L	V_{zz}	C_q
A	8-6411G31*d*	8-6311G*	6-11G[c]	1822	−1.48	14
B	8-6411G31*d*	8-63111G*	6-11G	1836	−1.51	15
C	8-6411G31*d*	8-63111G(2*d*)	6-11G	1848	−1.72	17
D	8-6411G31*d*	8-63111G(2*d*)	7-11G[d]	1854	−2.22	21
E	8-6411G31*d*	8-63111G(2*d*)	13*s*,3*sp*[e]	1854	−2.16	21
F	8-6411G31*d*	8-63111G(2*d*)	7-11G*	1857	−3.43	33

[a]Taken from Ref. 50.
[b]Inner 8-63 core taken from Ref. 52; outer exponents have been optimized, Table II.
[c]Taken from Refs. 12 and 53.
[d]Inner 7*s* core taken from Ref. 54; outer exponents have been optimized, Table II.
[e]Taken from Ref. 55; the three most diffuse *s* functions were removed and the three remaining most diffuse *s* shells were augmented by *p* shells.

TABLE II. Optimized orbital exponents of the uncontracted Gaussian functions.

	Sulfur[a]			Lithium[b]	
Shell	8-6311G*	8-63111G*	8-63111G(2*d*)	7-11G	7-11G*
sp	0.395	0.541	0.541	0.922	0.922
sp	0.160	0.260	0.260	0.193	0.193
sp		0.091	0.091		
d	0.352	0.352	1.705		0.179
d			0.354		

[a]Inner 8-63 core taken from Ref. 52.
[b]Inner 7*s* core taken from Ref. 54.

31(2) kHz (cf. Table IV). Thus the previously reported importance of polarization functions for EFG calculations with LCAO methods[28] is more confirmed.

A further extension of basis (F) with diffuse functions lead to severe SCF problems with CRYSTAL03 and was therefore discarded. Regarding the small energy differences between basis (D) and (F) it was concluded that basis set convergence was almost obtained. The optimized basis set (F) was then used for the subsequent field gradient calculations for the other methods and Li contents.

B. $LiTiS_2$

First, we studied in more detail *h*-$LiTiS_2$ with Li occupying either octahedral [Li_{oct}, Fig. 3(a)] or tetrahedral [Li_{tet}, Fig. 3(b)] interstitial positions. The lattice parameters *a* and *c* and all internal degrees of freedom, z_S for Li_{oct} and z_S, $z_{S'}$, z_{Li} for Li_{tet}, respectively, were optimized with each method. The system has an odd number of electrons per unit cell. The corresponding doublet ground state was treated with the unrestricted Kohn-Sham (UKS) formalism. Irrespective of the method the unpaired electron was found to be localized in the 3*d* shell of the Ti atom.

In Table III the structural parameters obtained at PWGGA, HFPW, and HF+PW level are compared with available experimental data.[59] In addition the lithium intercalation energy E_I with respect to TiS_2 and gas phase Li atoms

$$E_I = E(LiTiS_2) - E(TiS_2) - E(Li,g) \quad (4)$$

is also given.

The agreement with experiment for the *a* and *c* lattice parameters of *h*-$Li_{oct}TiS_2$ is similar for the PWGGA and HFPW methods, with deviations of +0.04 Å and −0.015 to −0.035 Å, while the HF+PW method underestimates both values, by −0.04 and −0.08 Å, respectively. All methods reproduce the experimental S fractional coordinate within 0.005. Our results slightly deviate from previous HF+PW calculations with CRYSTAL95.[12] In the latter study deviations of the *a* and *c* lattice parameters of −0.085 and −0.118 Å were obtained at HF+PW level, and of +0.042 and +0.094 Å at HF level. The difference can be explained by the different basis sets and the different treatment of correlation in CRYSTAL95 and CRYSTAL03. In CRYSTAL03 the numerical accuracy of the DFT integration procedure has been considerably improved compared to previous versions.

The local environment of Li_{oct} slightly deviates from the ideal octahedral symmetry. At PWGGA level the optimized

TABLE III. Optimized lattice parameters *a*,*c* (Å), S and Li fractional coordinates z_S, z_{Li}, and Li intercalation energies E_I (kJ/mol) for $LiTiS_2$ with Li placed at octahedral (Li_{oct}) and tetrahedral (Li_{tet}) interstitial sites; results obtained with the PWGGA, HFPW, and HF+PW methods using basis set F; for comparison the corresponding experimental results (Ref. 59) are given.

	Li_{oct}					Li_{tet}				
Parameter	*a*	*c*	z_S	z_{Li}	E_I	*a*	*c*	$z_S, z_{S'}$	z_{Li}	E_I
PWGGA[a]	3.497	6.173	0.235	0.500	−329	3.525	6.450	0.221, −0.225	−0.424	−307
HFPW[b]	3.496	6.153	0.233	0.500	−337	3.527	6.438	0.210, −0.230	−0.427	−320
HF+PW[c]	3.420	6.104	0.233	0.500	−288	3.452	6.360	0.210, −0.234	−0.430	−264
Expt.	3.459	6.188	0.238	0.500						

[a]PWGGA=Perdew-Wang exchange correlation functional (Ref. 56).
[b]HFPW=Hartree-Fock Perdew-Wang hybrid exchange functional plus Perdew-Wang correlation (Ref. 57).
[c]HF+PW=Hartree-Fock exchange plus Perdew-Wang correlation (Ref. 57).

TABLE IV. Calculated electric field gradient V_{zz} (a.u.$\times 10^3$) at Li position at optimized lattice parameters (with basis set F) and estimated ^{7}Li quadrupole coupling constants C_q (kHz) in h-$LiTiS_2$; Li is placed either in an octahedral (Li_{oct}) or a tetrahedral (Li_{tet}) interstitial site.

	Li_{oct}		Li_{tet}	
Method	V_{zz}	C_q	V_{zz}	C_q
PWGGA	−3.30	32	−8.83	85
HFPW	−2.72	26	−11.82	114
HF+PW	−3.00	29	−9.90	95
Expt.	31(2)[a]; 29[b]; 29[c]; ≈36[d]			

[a]This work (T=158 K); C_q=29.5(5) kHz (373K).
[b]Reference 41 (100 K≤T≤298 K).
[c]References 36 and 40 (room temperature).
[d]Reference 39 (233 K≤T≤296 K).

distance between the S layers is with 3.29 Å 9.7% larger than $2R/\sqrt{3}$ with R being the Li-S distance, 2.60 Å. This reduces the local symmetry from O_h to D_{3d}. The $Li_{tet}TiS_2$. lattice parameters are quite different from $Li_{oct}TiS_2$. The Ti-Ti interlayer distance given by the lattice parameter c is increased by 4.2%–4.6%, depending on the method, and also a increases by 0.8%–0.9%. The local Li_{tet} coordination has C_{3v} symmetry with one short Li-$S_{(1)}$ bond (2.29 Å at PWGGA level) and three Li-$S_{(2)}$ bond lengths of 2.40 Å. The two sulfur layers have slightly different distances from the Ti layers and therefore the two sulfur atoms, S and S' in Table III, are not equivalent.

It is generally assumed that Li occupies the octahedral interstitials rather than the tetrahedral sites.[36,39,59] This is confirmed by the present theoretical calculations. Besides the close agreement of the calculated and measured structural parameters only for $Li_{oct}TiS_2$, also the intercalation energy E_I is larger for Li_{oct} than for Li_{tet} (Table III). Almost independent of the method the difference $E_I(Li_{oct})-E_I(Li_{tet})$ is about −20 kJ/mol. The calculations refer to 0 K and do therefore not take into account entropy contributions to ΔG. But since there is no global change in the crystal structure between the two arrangements, it is assumed that $\Delta S_{oct\rightarrow tet}$ is small compared to ΔH which is approximated by the calculated ΔE_I. It has been suggested that the tetrahedral position is a transition structure for Li hopping between two octahedral positions.[13] Interestingly, the theoretically obtained energy difference $|E_I(Li_{tet})-E_I(Li_{oct})|$, 20 kJ/mol, is in the range of experimentally obtained activation energies from NMR results for Li diffusion in Li_xTiS_2, 20–30 kJ/mol.[4] It has to be noted, however, that the calculated ΔE_I corresponds to a displacement of all Li atoms in the lattice which is different from the situation during the diffusion process.

For the optimized lattice structures, all three methods, PWGGA, HFPW, and HF+PW, give rather similar values for the principal EFG component V_{zz} (Table IV). The differences, $3-6\times10^{-4}$ a.u., are within the changes due to basis set variations. The obtained quadrupole coupling constants C_q [Eq. (3)] range from 26 to 32 kHz and are in excellent agreement with the experimental values of 29 kHz (Ref. 41) and 31(2) kHz (cf. Table IV). For the PWGGA method, the ^{7}Li quadrupole coupling constant calculated with the optimized lattice structure, 32 kHz, does not significantly differ from the corresponding value with experimental lattice parameters, 33 kHz (Table I). This is mostly due to the relatively small differences between calculated and experimental lattice parameters. It has to be noted, however, that the effect of structure optimization on the calculated C_q is more pronounced for the tetrahedral position. With optimized lattice parameters, the calculated C_q at the tetrahedral Li position is 3–4 times larger, Table IV. Here the variation between the methods is larger than for Li_{oct}. But irrespective of the method used there is a clear distinction between the two positions which allows identification of the Li position by comparison with experiment. If instead the experimental lattice vectors and atomic positions are taken without optimization, C_q at octahedral and at tetrahedral sites are almost indistinguishable. This demonstrates the importance of geometry optimization for the calculation of EFG.

In order to investigate the difference of C_q between Li_{oct} and Li_{tet} experimentally, we plan to populate the tetrahedral position by increasing x in Li_xTiS_2 to values larger than 1. In that case the NMR signal from Li atoms at tetrahedral sites can be expected to be detectable. Since there is only one octahedral interstitial position for each Li atom, tetrahedral positions must be populated for $x>1$ if no lattice distortion occurs. For h-TiS_2 Li-naphthalide has been successfully applied to intercalate lithium in mole fractions up to x=1.49.[60]

C. $Li_{0.67}TiS_2$

In order to simulate smaller Li contents $x=2/3$ and $x=1/3$ a supercell with transformation matrix $\mathbf{L}$ was constructed from the primitive unit cell,

$$\mathbf{L}=\begin{pmatrix}1 & 2 & 0\\ 2 & 1 & 0\\ 0 & 0 & 1\end{pmatrix}. \tag{5}$$

The volume of the supercell is $|\det \mathbf{L}|=3$ times larger than that of the primitive cell. For $Li_{0.67}TiS_2$ calculations a Li atom was placed at $(00\frac{1}{2})$ in the primitive cell and one of the three Li atoms in the supercell was then removed. The lattice parameters a and c and all atomic positions were optimized with CRYSTAL03. The vectors were optimized using numerical gradients, and the fractional coordinates were relaxed using analytical gradients and an updated Hessian method.[48] No disordering along the c axis was taken into account as found experimentally.[59] The results for the optimized lattice parameters a and c, the intercalation energy E_I and the field gradient component V_{zz} are presented in Table V for Li placed at octahedral and tetrahedral sites. In the case of Li_{tet} two equivalent positions were selected in order to increase the symmetry. With all three methods, PWGGA, HFPW, and HF+PW, the optimized lattice parameters are smaller than for x=1.0, in accordance with experiments.[36,59] For Li_{oct}, c is

TABLE V. Optimized lattice parameters a,c (Å), Li intercalation energies E_I (kJ/mol), and estimated ^{7}Li quadrupole coupling constants C_q (kHz) for $Li_{0.67}TiS_2$ with Li placed at octahedral (Li_{oct}) or tetrahedral (Li_{tet}) interstitial sites; results obtained with the PWGGA, HFPW, and HF+PW methods using basis set F; for comparison the corresponding experimental results (Ref. 59) are given.

	Li_{oct}				Li_{tet}			
Parameter	a	c	E_I	C_q	a	c	E_I	C_q
PWGGA	3.436	6.114	−338	18	3.451	6.406	−317	88
HFPW	3.406	6.099	−314	21	3.440	6.365	−296	95
HF+PW	3.419	5.932	−238	13	3.417	6.068	−231	66
Expt.	3.43	6.17		11(2);[a] 13;[b] ≈26[c]				

[a]This work, $Li_{0.7}TiS_2$ (T=143 K); C_q=12.6(2) kHz (293 K), C_q=14.8(5) kHz (373 K).
[b]Reference 41, $Li_{0.7}TiS_2$ (100 K≤T≤298 K).
[c]References 36 and 39 (233 K≤T≤296 K).

decreased by 0.9%–1.0%, and a is decreased by 1.7%–2.6% at PWGGA and HFPW level. With the HF+PW approach, the decrease of c, by 2.8%, is more pronounced whereas a is almost unchanged. A similar change of the lattice parameters with decreasing x is obtained for Li_{tet}.

Energetically, lithium intercalation at the octahedral position is more stable than at the tetrahedral interstitial. $E_I(Li_{oct})-E_I(Li_{tet})$ is with −18 and −21 kJ/mol similar as for x=1 with PWGGA and HFPW, while it is only −7 kJ/mol at HF+PW level.

With all three methods the calculated quadrupole coupling constant C_q is much smaller for x=0.67 than for x=1. The range of C_q for Li_{oct}, 13–21 kHz, is again in close agreement with our experimental value of about 11(2) kHz at 143 K and experimental results found in the literature, 13 kHz (100 K–300 K) (Ref. 41) and 12.6 kHz (298 K).[42] The quadrupole coupling constant at Li_{tet} position is about 5 times larger than for Li_{oct}, irrespective of the method. Thus it is possible to distinguish between the two positions also at smaller Li content.

D. $Li_{0.33}TiS_2$

The same supercell as described in the previous section was used to model x=0.33. In the $Li_3Ti_3S_6$ supercell two of the three Li atoms were removed. Therefore an odd total number of electrons per supercell was obtained which lead to a doublet electronic state. This was treated with the UKS formalism. Some test calculations were performed using the restricted open-shell Kohn-Sham (ROKS) formalism, which gave similar results. A full optimization of lattice parameters and atomic coordinates was performed in a way similar to that described in the previous subsection. The results for structural, energetic and electronic properties obtained with PWGGA, HFPW, and HF+PW are summarized in Table VI. At variance with experimentally observed trends,[36,59] the lattice parameters for Li_{oct} are not further decreased when the content is decreased from 0.67 to 0.33. On the other hand, there is a substantial lattice contraction for Li_{tet} with all three methods.

The difference between the intercalation energies for octahedral and tetrahedral Li positions at x=0.33 is larger than

TABLE VI. Optimized lattice parameters a,c (Å), Li intercalation energies E_I (kJ/mol), and estimated ^{7}Li quadrupole coupling constants C_q (kHz) for $Li_{0.33}TiS_2$ with Li placed at octahedral (Li_{oct}) or tetrahedral (Li_{tet}) interstitial sites; results obtained with the PWGGA, HFPW, and HF+PW methods using basis set F; for comparison the corresponding experimental results are given.

	Li_{oct}				Li_{tet}			
	a	c	E_I	C_q	a	c	E_I	C_q
PWGGA	3.437	6.129	−349	1	3.420	6.190	−322	54
HFPW	3.433	6.031	−344	5	3.387	6.053	−296	44
HF+PW	3.430	6.144	−462	−46	3.430	5.905	−382	26
Expt.	3.42[a]	6.11[a]		<5[b]; ≈10[c]				

[a]Reference 59, h-$Li_{0.33}TiS_2$.
[b]This work, h-$Li_{0.3}TiS_2$ (T=373 K).
[c]Reference 39, h-$Li_{0.33}TiS_2$ (233 K≤T≤296 K), and Ref. 36, h-$Li_{0.3}TiS_2$ (room temperature).

TABLE VII. Optimized lattice parameters a,c (Å), intercalation energies Li E_I (kJ/mol), and estimated ^{7}Li quadrupole coupling constants C_q (kHz) for $Li_{0.25}TiS_2$ with Li placed at octahedral (Li_{oct}) or tetrahedral (Li_{tet}) interstitial sites; results obtained with the PWGGA, HFPW, and HF+PW methods using basis set F; for comparison the corresponding experimental results are given.

	Li_{oct}				Li_{tet}			
	a	c	E_I	C_q	a	c	E_I	C_q
PWGGA	3.425	6.242	−350	6	3.471	6.306	−309	84
HFPW	3.447	6.162	−346	14	3.444	6.356	−325	81
HF+PW	3.434	6.049	−453	−50	3.505	5.926	−416	21
Expt.	3.42[a]	6.11[a]		<5[b]; ≈ 7[c]				

[a]Reference 59, h-$Li_{0.33}TiS_2$.
[b]This work, h-$Li_{0.3}TiS_2$ ($T=373$ K).
[c]Reference 39, h-$Li_{0.25}TiS_2$ (233 K$\leqslant T\leqslant$296 K), and Ref. 36, h-$Li_{0.2}TiS_2$ (room temperature).

at $x=0.67$ and $x=1.0$. It ranges between −27 kJ/mol (PWGGA) and −80 kJ/mol (HF+PW).

The calculated field gradients and therefore C_q become quite small at $x=0.33$ with PWGGA and HFPW, 1 and 5 kHz, respectively. This is only slightly smaller than the experimental value of about 7(2) kHz (Ref. 42) and in agreement with our experimental result, that C_q of $Li_{0.33}TiS_2$ is estimated to be less than 5 kHz (cf. Fig. 1). At HF+PW level, however, a large but negative value, −46 kHz, is obtained for Li_{oct} C_q. The large change of the field gradient and intercalation energy between $x=0.67$ and $x=0.33$ at this level of theory is probably due to the electronic structure obtained with HF+PW. At this level the unpaired electron of the $^2LiTi_3S_6$ supercell is strongly localized in the 3d shell of one Ti atom. This localization leads to a perturbation of the electric field compared to the supercell with larger Li content. At the PWGGA and HFPW levels, the spin localization is much less pronounced. The spin densities ϱ_s at the three Ti atoms are 0.4 (0.45), 0.3 (0.22), and 0.3 (0.22) with PWGGA (HFPW). ϱ_s is defined as the difference between the total densities of spin-up and spin-down electrons. At the tetrahedral position the quadrupole coupling constant is considerably more positive than at octahedral position for all three methods. Similar as for the higher Li contents, the agreement of calculated field gradients and structural parameters with the measured values is much closer for the octahedral site than for the tetrahedral site. Together with the larger intercalation energy for Li_{oct} this is a clear indication that Li insertion into TiS_2 occurs at the octahedral sites even at smaller Li mole fractions.

E. $Li_{0.25}TiS_2$

The smallest Li content of $x=0.25$ considered in the present study was modeled with a supercell generated by the following transformation matrix **L**,

$$\mathbf{L}=\begin{pmatrix}2&0&0\\0&2&0\\0&0&1\end{pmatrix}. \quad (6)$$

In the $Li_4Ti_4S_8$ supercell three of the four generated Li atoms were removed. Similar as for $x=0.33$ this corresponds to an odd number of electrons and a doublet electronic state which was again treated at the UKS level of theory. The results are presented in Table VII. They correspond to fully optimized structures as for the other compositions.

The experimentally observed trend of monotonically decreasing lattice parameters a and c with decreasing lithium content is not found theoretically. This is not due to an erroneous description of the lithium-free structure of TiS_2 as shown in Table VIII. In particular for the HFPW method the calculated structural parameters agree within 0.015 Å with experimental data. Nevertheless, the c parameters for $x=1.0$(6.153 Å), 0.67(6.099 Å), 0.33(6.031 Å), 0.25(6.162 Å) obtained with HFPW do not decrease monotonically. Similar deviations are observed for the other methods.

Similar as for the larger Li contents, the intercalation energy is larger at the octahedral position than at the tetrahedral site. The difference $E_I(Li_{oct})-E_I(Li_{tet})$ generally increases with decreasing x for all three approaches. But the increase is in no case monotonic.

A similar observation is made for the field gradient. The smallest values are obtained for $x=0.33$. For the smallest considered Li mole fraction $x=0.25$ there is again an in-

TABLE VIII. Optimized lattice parameters a,c (Å) for TiS_2; results obtained with the PWGGA, HFPW, and HF+PW methods using basis set F; for comparison the corresponding experimental results (Ref. 59) are given.

Parameter	a	c
PWGGA	3.434	5.669
HFPW	3.423	5.688
HF+PW	3.409	5.588
Expt.	3.408	5.699

crease of C_q with PWGGA and HFPW. This trend has also been observed experimentally[39] for Li contents $x<0.2$ and attributed to charge transfer from Li to Ti. The charge transfer is observed in the present calculations and leads to an increased spin density in the 3*d* shells of Ti atoms. At PWGGA and HFPW level, the spin density is not evenly distributed among the four Ti atoms in the cell although there is not a full localization on one Ti atom. The anisotropic electron distribution increases the electric field gradient at Li position and leads to a larger C_q than for $x=0.33$. Similar as for $x=0.33$, the EFG obtained with HF+PW is strongly negative, in disagreement with experiment (Table VII). Again this can be attributed to the strong spin localization obtained with this approach which is probably an artefact.

V. CONCLUSIONS

Periodic calculations of electric field gradients with wave functions based on atom-centered basis functions reproduce experimental quadrupole coupling constants of ^{7}Li in $LiTiS_2$ within a few kHz. The accuracy of the theoretical results is determined by the quality of the atomic basis sets. A procedure to obtain convergence based on energetic properties is presented. The differences between field gradients obtained with pure DFT methods and HF-DFT hybrid methods are small. This is different from earlier studies of transition metal compounds where large deviations between DFT- and HF-based methods were found. The only exception is the HF+PW approach where the HF exchange is combined with a correlation functional. At small Li contents a strong localization of the unpaired electron at a single Ti atom is obtained which leads to a perturbation of the electric field and to field gradients that do not correspond to experiment. With all three methods under consideration the calculated field gradients of Li at octahedral and tetrahedral sites are different due to the different local environment. This allows for identification of the Li position in cases where no experimental information is available.

ACKNOWLEDGMENTS

This work has been supported by Deutsche Forschungsgemeinschaft within the Priority Programme 1136 "Substitution effects in ionic solids." We are grateful to A. Payer and R. Schöllhorn for leaving us the samples.

[1] *Lithium Ion Batteries*, edited by M. Wakihara and O. Yamamoto (Wiley-VCH, Weinheim, 1998).
[2] M.S. Whittingham, Prog. Solid State Chem. **12**, 41 (1978).
[3] M.S. Whittingham, R. Chen, T. Chirayil, and P. Zavalij, Solid State Ionics **94**, 227 (1997).
[4] W. Küchler, P. Heitjans, A. Payer, and R. Schöllhorn, Solid State Ionics **70**, 434 (1994).
[5] L. Bernard, W. Glaunsinger, and P. Colombet, Solid State Ionics **17**, 81 (1985).
[6] C. Umrigar, D.E. Ellis, D.-S. Wang, H. Krakauer, and M. Posternak, Phys. Rev. B **26**, 4935 (1982).
[7] C. Julien, I. Samaras, O. Gorochov, and A.M. Ghorayeb, Phys. Rev. B **45**, 13390 (1992).
[8] J. Chen, Z.L. Tho, and S.L. Li, Angew. Chem., Int. Ed. **42**, 2147 (2003).
[9] R. Winter and P. Heitjans, Nanostruct. Mater. **12**, 883 (1999).
[10] R. Winter and P. Heitjans, J. Phys. Chem. B **105**, 6108 (2001).
[11] P. Heitjans and S. Indris, J. Phys.: Condens. Matter **15**, R1257 (2003).
[12] D.G. Clerc, R.D. Poshusta, and A.C. Hess, J. Phys. Chem. A **101**, 8926 (1997).
[13] F. Mendizábal, R. Contreras, and A. Aizman, J. Phys.: Condens. Matter **9**, 3011 (1997).
[14] Y.S. Kim, Y. Koyama, I. Tanaka, and H. Adachi, Jpn. J. Appl. Phys., Part 1 **37**, 6440 (1998).
[15] M.K. Aydinol, A.F. Kohan, G. Ceder, K. Cho, and J. Joannopoulos, Phys. Rev. B **56**, 1354 (1997).
[16] H. Ennamiri, R. Nassif, Y. Boughaleb, and J.F. Gouyet, J. Phys.: Condens. Matter **9**, 2433 (1997).
[17] L. Benco, J.L. Barras, M. Atanasov, C. Daul, and E. Deiss, J. Solid State Chem. **145**, 503 (1999).
[18] A. Abragam, *The Principles of Nuclear Magnetism* (Clarendon, Oxford, 1961).
[19] M.H. Cohen and F. Reif, in *Solid State Physics*, edited by F. Seitz and D. Turnbull (Academic, New York, 1957), Vol. 5, p. 321.
[20] T.P. Das and E.L. Hahn, *Nuclear Quadrupole Resonance Spectroscopy, Solid State Phys. Suppl. 1*, edited by F. Seitz and D. Turnbull (Academic, New York, 1958).
[21] P.L. Bryant, C.R. Harwell, K. Wu, F.R. Fronczek, R.W. Hall, and L.G. Butler, J. Phys. Chem. A **103**, 5246 (1999).
[22] E.P. Stoll, P.F. Meier, and T.A. Claxton, Phys. Rev. B **65**, 064532 (2002).
[23] G. Frantz, H. Dufner, and P.C. Schmidt, Z. Naturforsch., A: Phys. Sci. **49**, 116 (1994).
[24] P. Dufek, P. Blaha, and K. Schwarz, Phys. Rev. Lett. **75**, 3545 (1995).
[25] P. Novák and F.R. Wagner, Phys. Rev. B **66**, 184434 (2002).
[26] M. Iglesias, K. Schwarz, P. Blaha, and D. Baldomir, Phys. Chem. Miner. **28**, 67 (2001).
[27] S. Lany, P. Blaha, J. Hamann, V. Ostheimer, H. Wolf, and T. Wichert, Phys. Rev. B **62**, R2259 (2000).
[28] E.A. Moore, C. Johnson, M. Mortimer, and C. Wigglesworth, Phys. Chem. Chem. Phys. **2**, 1325 (2000).
[29] F. Hagelberg, T.P. Das, and K.C. Mishra, Phys. Rev. B **65**, 014425 (2001).
[30] M.H. Palmer and J.A. Blair-Fish, Z. Naturforsch., A: Phys. Sci. **49**, 137 (1994).
[31] P. Schwerdtfeger, T. Söhnel, M. Pernpointner, J.K. Laerdahl, and F.E. Wagner, J. Chem. Phys. **115**, 5913 (2001).
[32] P. Schwerdtfeger, M. Pernpointner, and J.K. Laerdahl, J. Chem. Phys. **111**, 3357 (1999).
[33] M. Bühl, Chem. Phys. Lett. **267**, 251 (1997).
[34] M. Kaupp, O.L. Malkina, and V.G. Malkin, J. Chem. Phys. **106**, 9201 (1997).

[35] P. Blaha, K. Schwarz, W. Faber, and J. Luitz, Hyperfine Interact. **126**, 389 (2000).
[36] B.G. Silbernagel and M.S. Whittingham, J. Chem. Phys. **64**, 3670 (1976).
[37] R.L. Kleinberg and B.G. Silbernagel, Solid State Commun. **36**, 345 (1980).
[38] R.L. Kleinberg, B.G. Silbernagel, and A.H. Thompson, Solid State Commun. **41**, 401 (1982).
[39] R.L. Kleinberg, J. Phys. Chem. Solids **43**, 285 (1982).
[40] B.G. Silbernagel, Solid State Commun. **17**, 361 (1975).
[41] C. Prigge, W. Müller-Warmuth, and R. Schöllhorn, Z. Phys. Chem. (Munich) **189**, 153 (1995).
[42] W. Küchler, Ph.D. thesis, Universität Hannover, 1993.
[43] H.W. Spiess, in *NMR Basic Principles and Progress*, edited by P. Diehl, E. Fluck, and R. Kosfeld (Springer, Berlin, 1978), Vol. 15, p. 55.
[44] M. Mehring, *Principles of High Resolution NMR in Solids*, 2nd ed. (Springer, Berlin, 1983).
[45] W. Müller-Warmuth, in *Progress in Intercalation Research*, edited by W. Müller-Warmuth and R. Schöllhorn (Kluwer, Dordrecht, 1994), pp. 339–455.
[46] P. Pyykkö, Mol. Phys. **99**, 1617 (2001).
[47] K. Eichele, WSolids1, Version 1.17.30, Universität Tübingen, 2001; http://casgm3.anorg.chemie.uni-tuebingen.de/klaus/soft/
[48] V.R. Saunders, R. Dovesi, C. Roetti, R. Orlando, C.M. Zicovich-Wilson, N.M. Harrison, K. Doll, B. Civalleri, I. Bush, Ph. D'Arco, and M. Llunell, CRYSTAL03 User's Manual, University of Torino, Torino, 2003; http://www.crystal.unito.it/
[49] W.J. Hehre, R. Ditchfield, and J.A. Pople, J. Chem. Phys. **56**, 2257 (1972).
[50] W.C. Mackrodt, E.A. Simson, and N.M. Harrison, Surf. Sci. **384**, 192 (1997).
[51] A. Lichanot, E. Aprà, and R. Dovesi, Phys. Status Solidi B **177**, 157 (1993).
[52] M. Mian, N.M. Harrison, V.R. Saunders, and W.R. Flavell, Chem. Phys. Lett. **257**, 627 (1996).
[53] L. Ojamäe, K. Hermansson, C. Pisani, M. Causà, and C. Roetti, Acta Crystallogr., Sect. B: Struct. Sci. **50**, 268 (1994).
[54] N. Godbout, D.R. Salahub, J. Andzelm, and E. Wimmer, Can. J. Chem. **70**, 560 (1992).
[55] H. Partridge, J. Chem. Phys. **90**, 1043 (1989).
[56] J.P. Perdew and Y. Wang, Phys. Rev. B **45**, 13244 (1992).
[57] T. Bredow and A.R. Gerson, Phys. Rev. B **61**, 5194 (2000).
[58] G. Klösters and M. Jansen, Solid State Nucl. Magn. Reson. **16**, 279 (2000).
[59] J.R. Dahn, W.R. McKinnon, R.R. Haering, W.J.L. Buyers, and B.M. Powell, Can. J. Phys. **58**, 207 (1980).
[60] W.B. Johnson and W.L. Worell, J. Electrochem. Soc. **133**, 1966 (1986).